Multimodal workflow for high-resolution imaging of individual skeletal muscle fibers using nano-DESI MSI

Daisy Unsihuay,[a] Hang Hu,[b] Jiamin Qiu,[c] Alessandra Latorre-Palomino,[d] Manxi Yang,[b] Feng Yue,[c] Ruichuan Yin, [a] Shihuan Kuang [c] and Julia Laskin*[b]

a. Department of Pathology and Laboratory Medicine, University of Pennsylvania, Philadelphia, PA, 19104, USA.
b. Department of Chemistry, Purdue University, West Lafayette, IN 47907, USA. Email: jlaskin@purdue.edu
c. Department of Animal Sciences, Purdue University, West Lafayette, IN 47907, USA.
d. Department of Chemistry, Universidad Nacional Mayor de San Marcos, Lima, Peru

Tables: Table can be found in supplemental file entitled: “supplemental tables.xlsx”

Table S1. Annotated species with their relative abundances extracted per each fiber type with their classification based on the pattern distribution and metabolism depicted across all the replicates.

Table S2. Heatmap displaying variation of the Z-scores across each fiber type and the three replicates of all annotated species.

Table S3. MS/MS results of the acyl chain profiling of all the phospholipids detected in GAS tissue

Additional images:

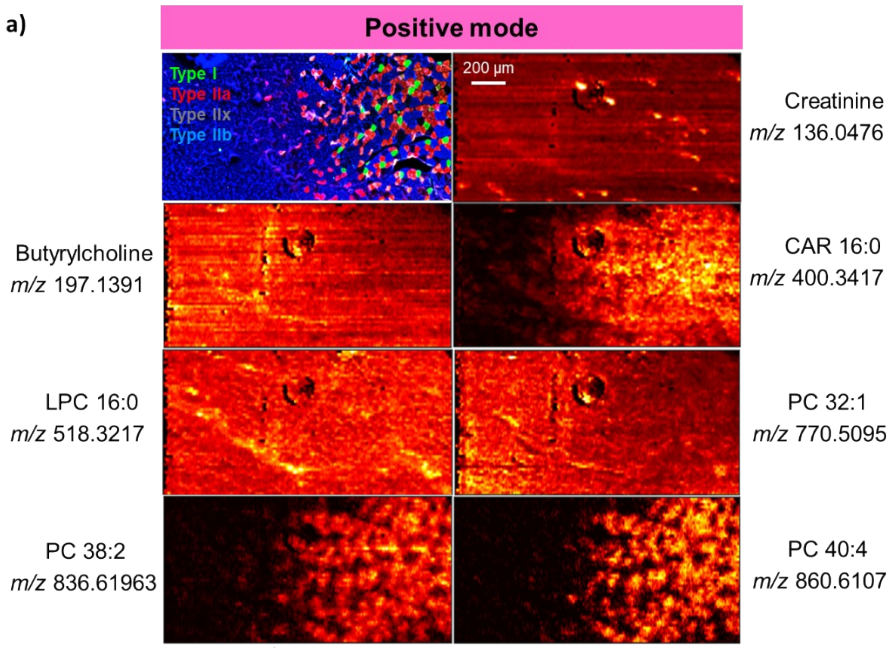
a)
Positive mode
Type I
Type IIa
Type IIx
Type IIb
200 µm
Creatinine
m/z 136.0476
Butyrylcholine
m/z 197.1391
CAR 16:0
m/z 400.3417
LPC 16:0
m/z 518.3217
PC 32:1
m/z 770.5095
PC 38:2
m/z 836.61963
PC 40:4
m/z 860.6107

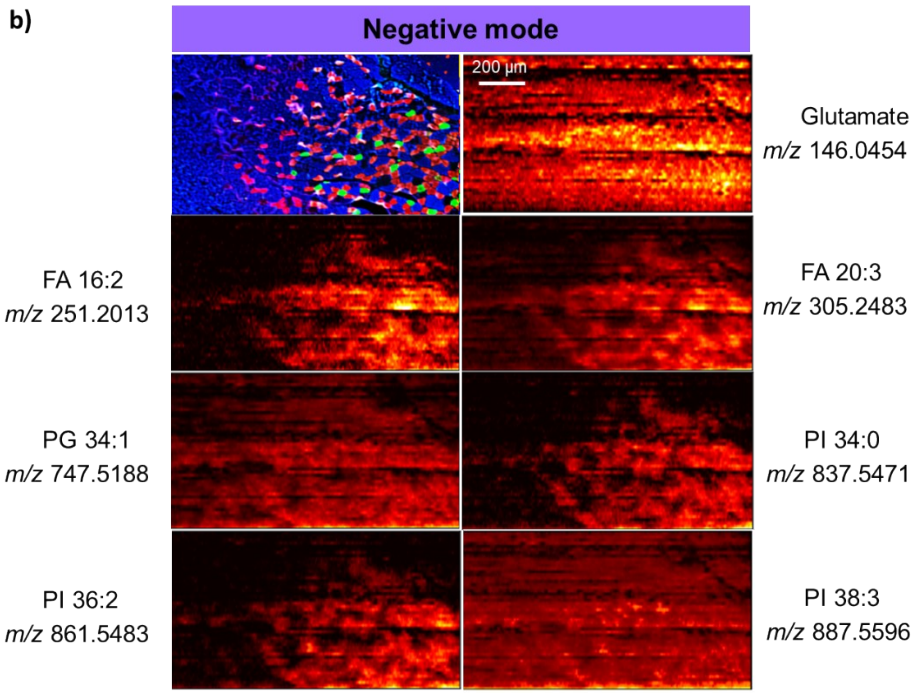

Figure S1. Representative nano-DESI ion images collected in mouse 1 in a) positive and b) negative mode.

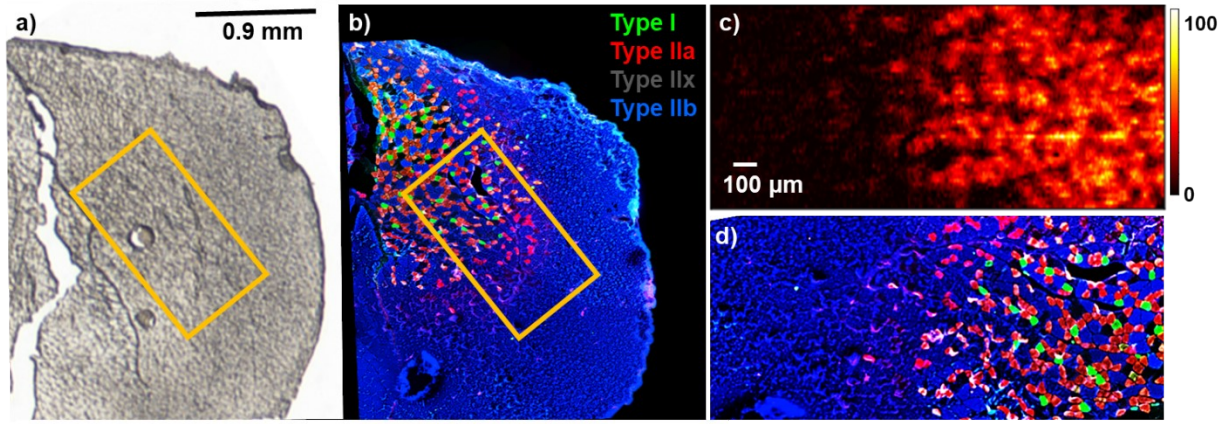

Figure S2. Multimodal imaging of muscle fibers. a) Optical image of GAS tissue . b) IF image collected on an adjacent section. The yellow boxes indicate the scanned region in MSI experiments. c) Ion image of m/z 856.5830. d) IF image of the region indicated by the yellow box. Scale bars are indicated inside the ion images. Color bar indicating relative abundances is displayed on the right of the ion image.

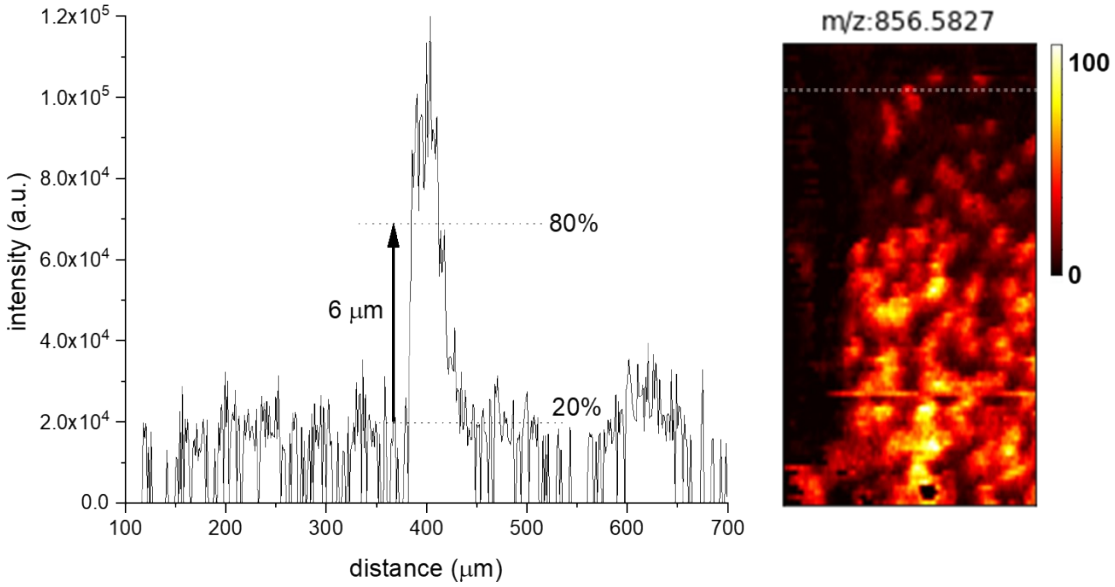

Figure S3. Calculation of the spatial registration of the imaging of individual muscle fibers. We use variations on the chemical gradient of a molecule using the 80/20 rule.

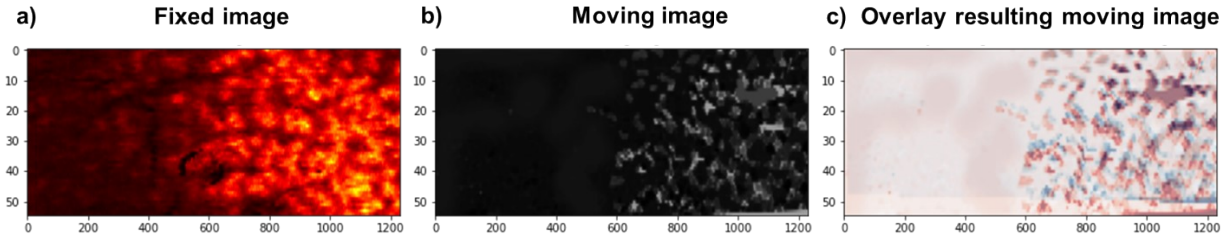

Figure S4. Affine registration process. a) Ion images that serves as the ion image, b) gray scale of the IF images which serves as the moving image. c) Result of the affine registration of IF image to the ion image.

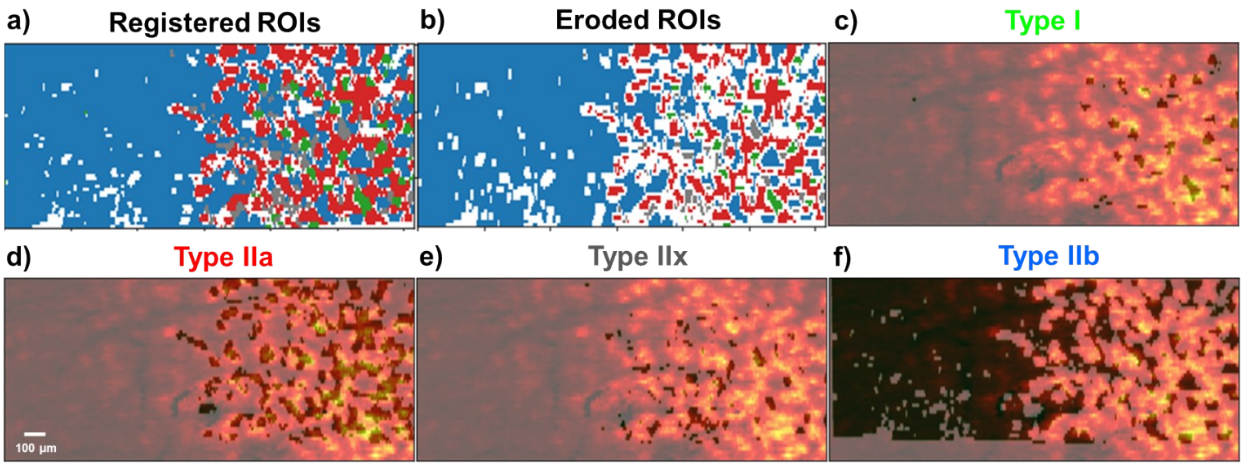

Figure S5. a) Segmented IF image. b) Eroded image of a) to eliminate surrounding pixels that might overlap with other fiber types. Fiber-specific mask generated for c) type I, d) type IIa, e) type IIx and f) type IIb are displayed overlapping a representative ion image to show the good matching of the mask and the fiber pattern.

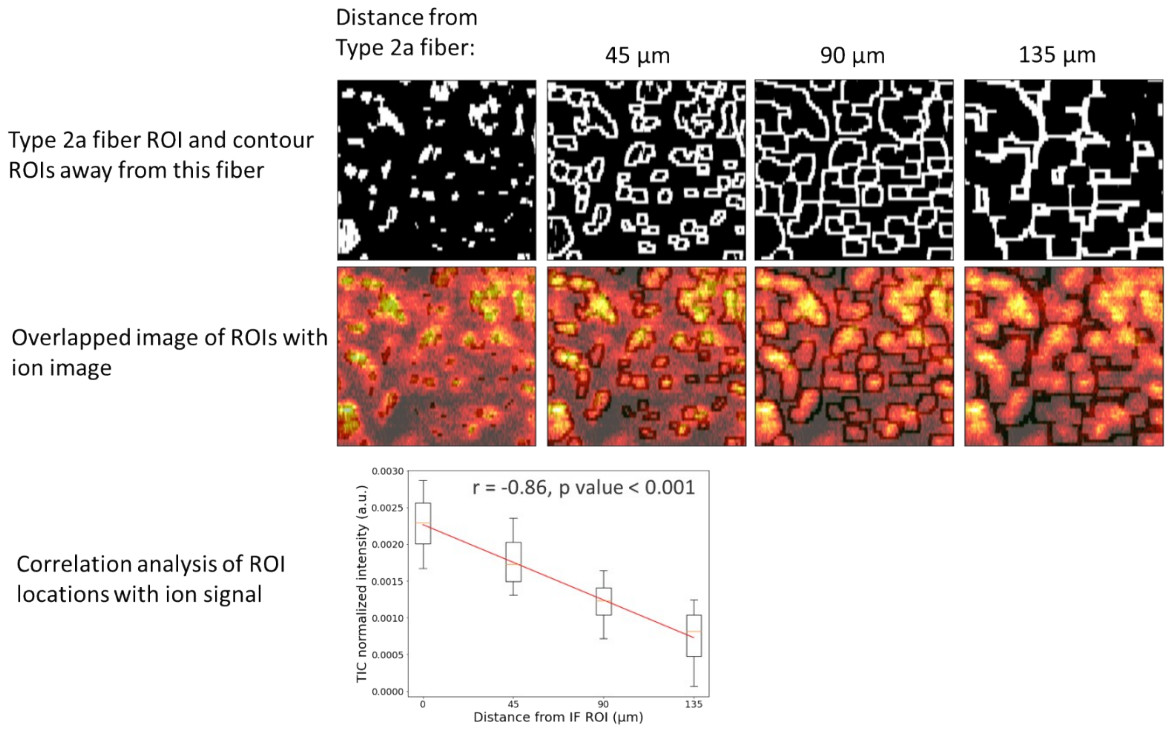

Figure S6. Correlation analysis of IF image type IIa locations with ion signal of m/z 856.5835. The type IIa fiber ROI (white color) is obtained using image registration and segmentation as demonstrated in Fig. 2. Contour ROIs (white color) with varying distance away from type IIa fiber ROI is generated by dilation morphology processing. Overlap images of ROIs and ion image are shown in the second row. Finally, the boxplots of ion signals in ROIs with varying spatial distance away from Type 2a fiber are overlapped with a linear regression line, which indicates a linear correlation between ion signal and tissue location distance away from IF image type IIa fiber. r = Pearson correlation coefficient. p value rejects null hypothesis that r = 0.

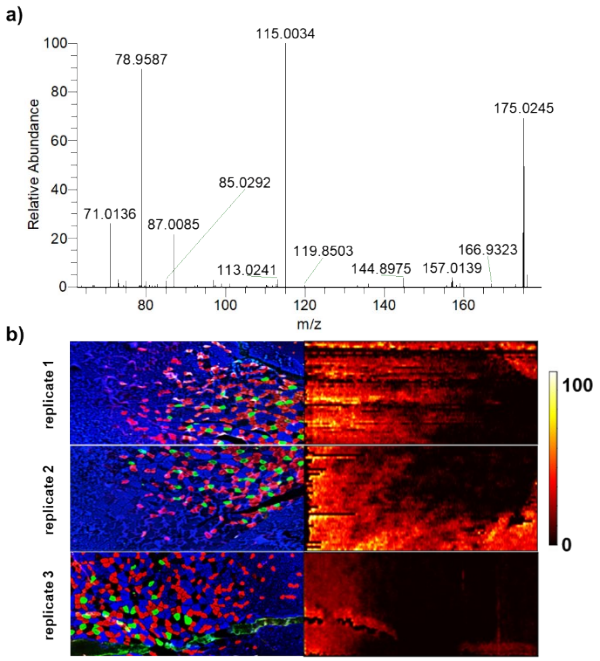

Figure S7. a) MS/MS spectrum of m/z 175.0245 identified as ascorbate. b) IF and TIC normalized ion images of *m/z* 175. 0245

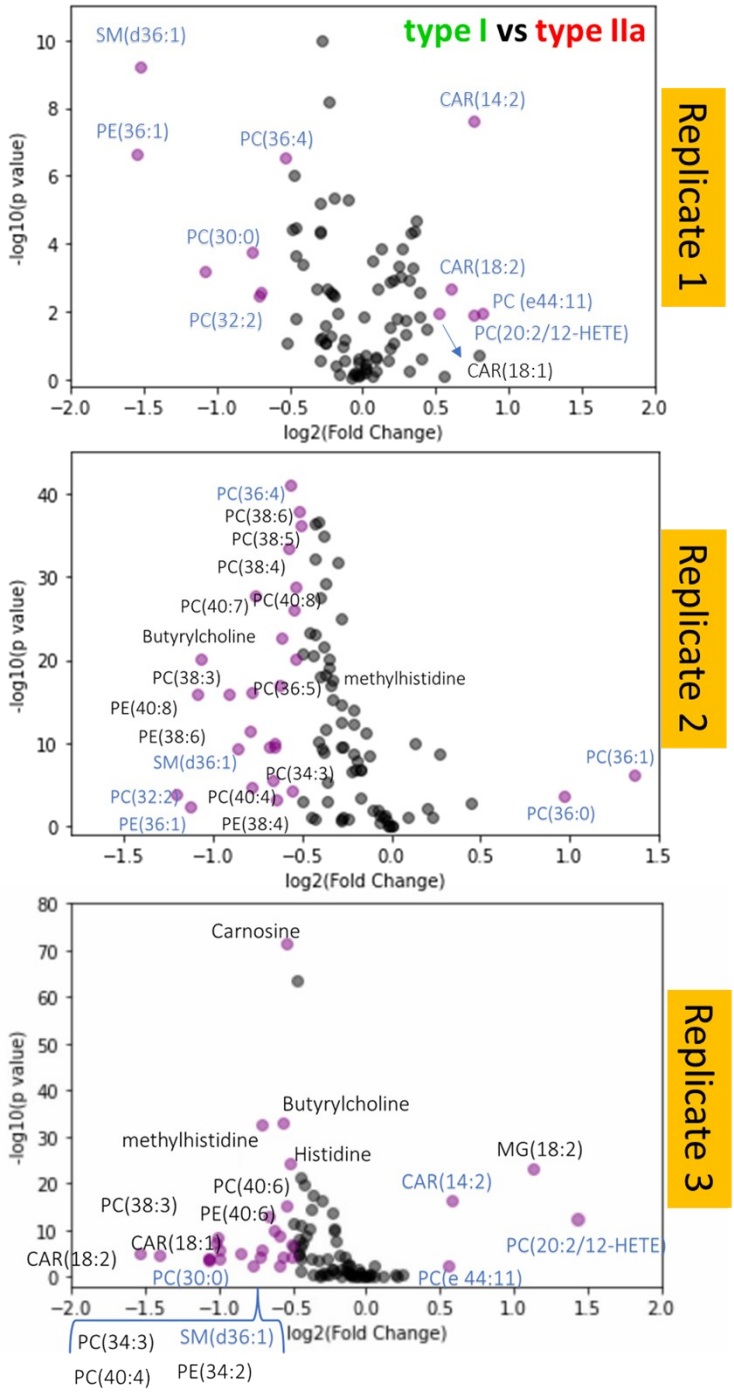

Figure S8. Volcano plots showing direct comparison of type I vs. type IIa across all replicates. Purple circles indicate molecules significantly different displaying a $\log_2$(FC) less than -0.5 or greater than 0.5 and p-value <0.05.

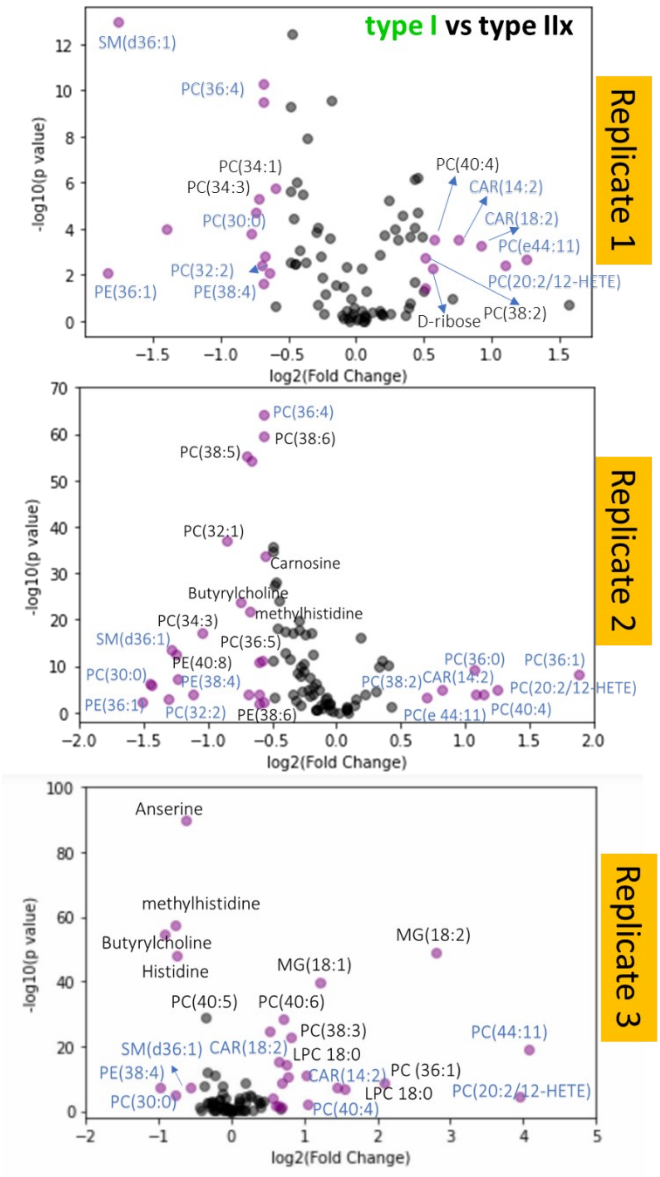

Figure S9. Volcano plots showing direct comparison of type I vs. type IIx. Purple circles indicate molecules significantly different displaying a $\log_2$(FC) less than -0.5 or greater than 0.5 and p-value <0.05.

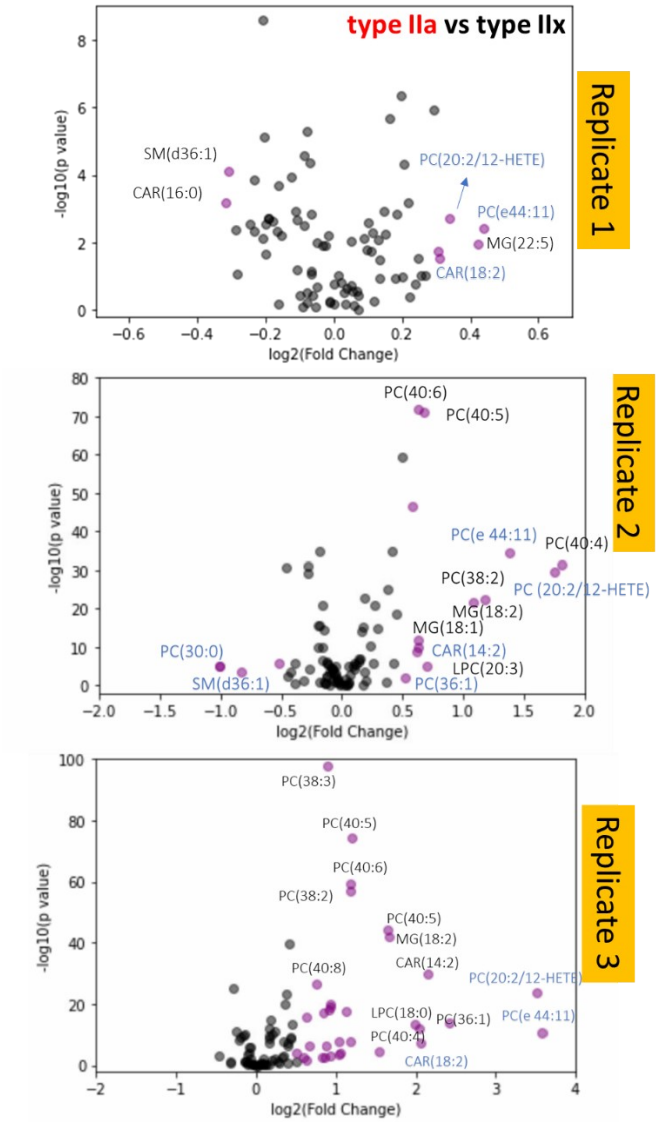

Figure S10. Volcano plots showing direct comparison of type IIa vs. type IIx. Purple circles indicate molecules significantly different displaying a $\log_2$(FC) less than -0.3 or greater than 0.3 and p-value <0.05 in replicate 1, and $\log_2$(FC) less than -0.5 or greater than 0.5 and p-value <0.05 in replicate 2 and 3.

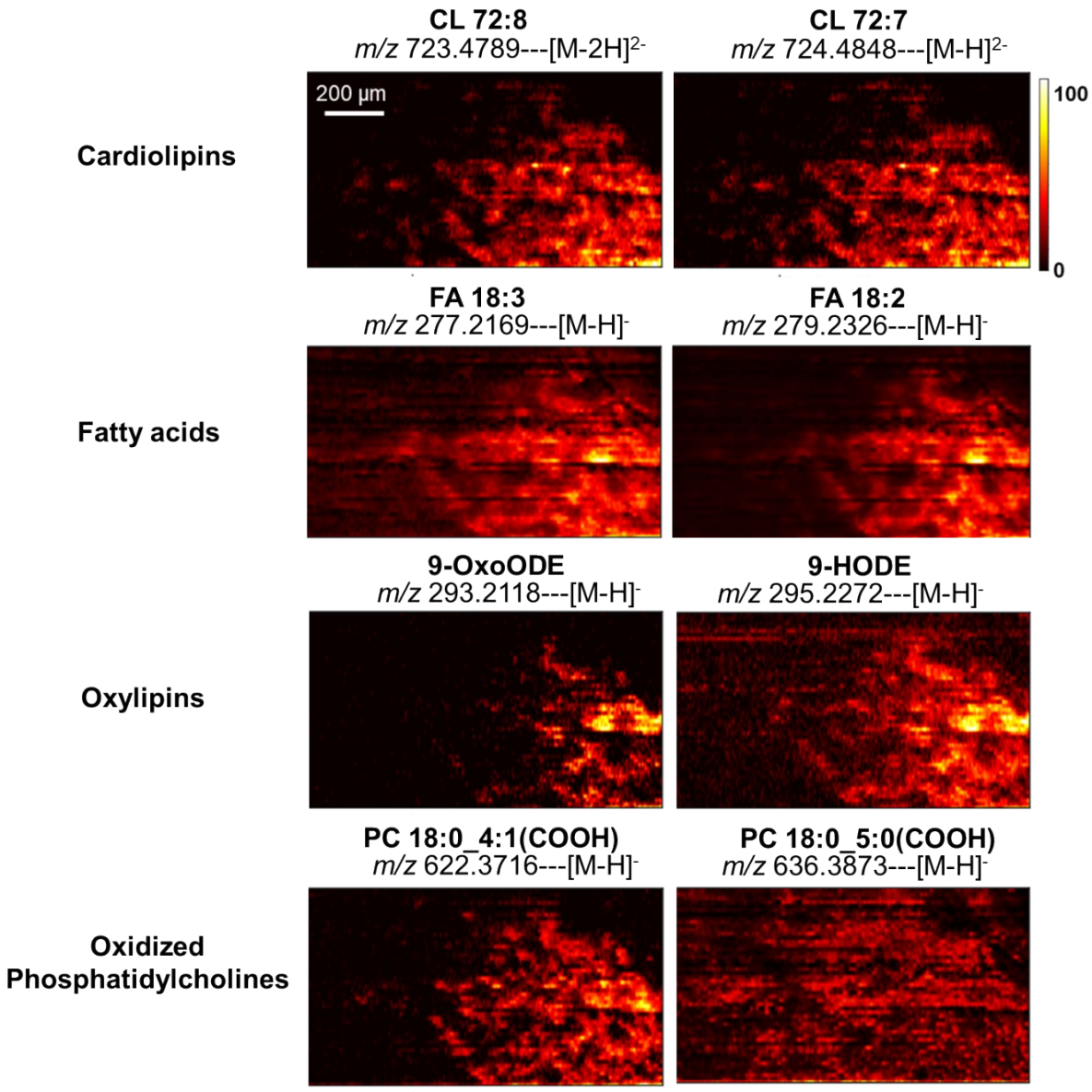

Figure S11. Representative ion images of different lipid classes detected in negative mode.

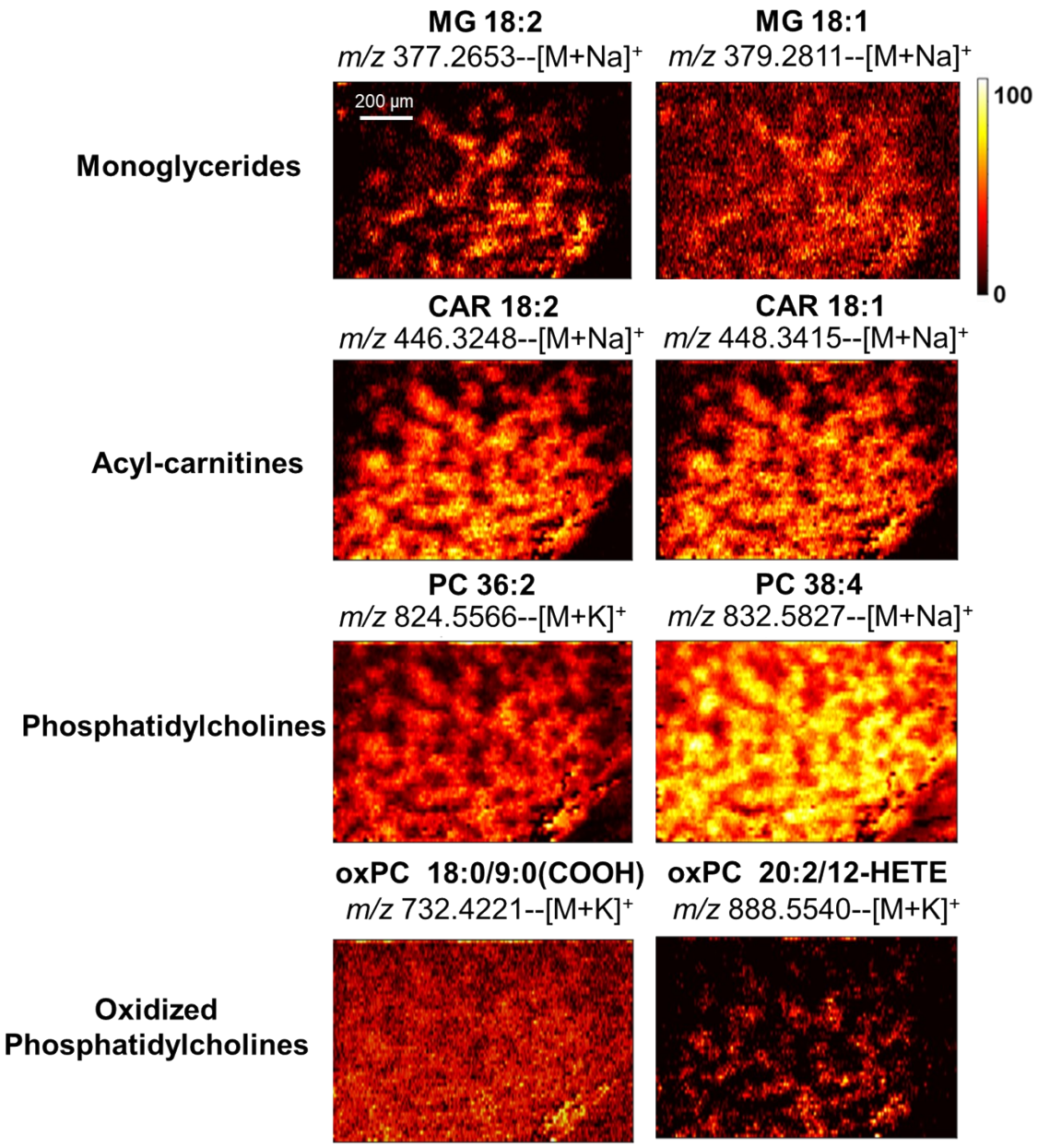

Figure S12. Representative ion images of different lipid classes detected in positive mode.

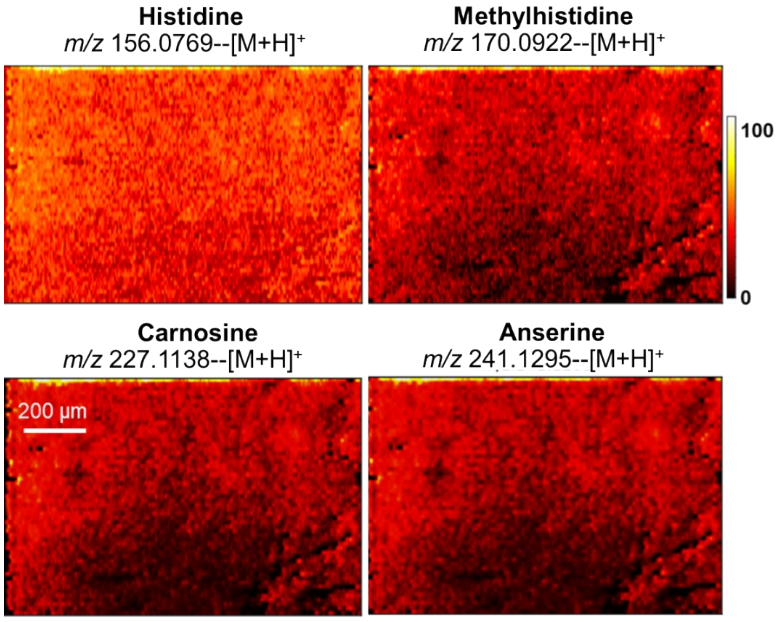

Figure S13. Ion images of histidine-related compounds which are enhanced in glycolytic fibers.

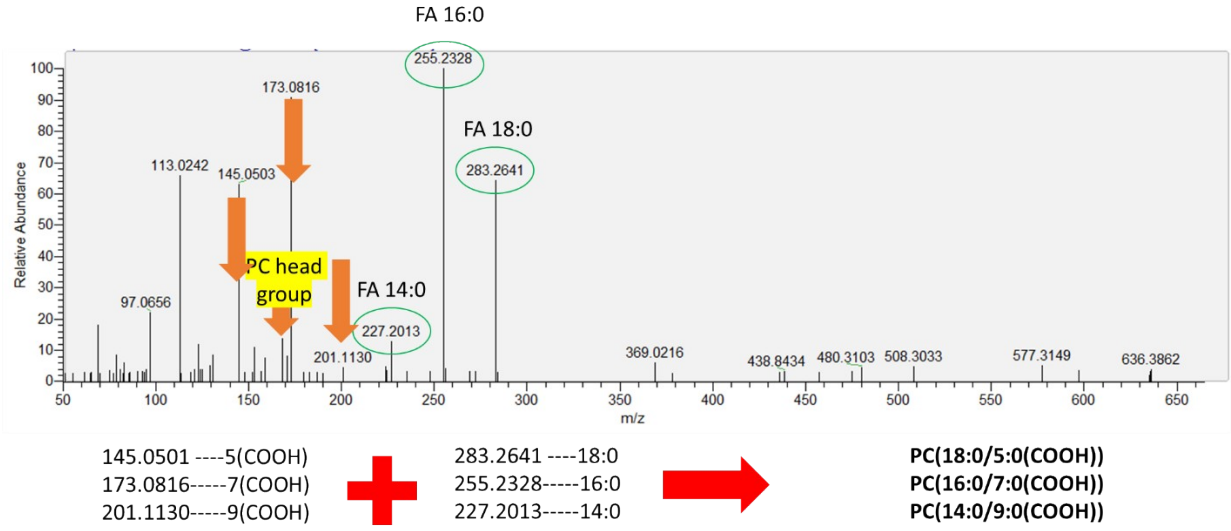

Figure S14. MS/MS spectrum of $[M-H]^-$ adduct of *m/z* 636.3862 showing the presence of multiple isomers. Orange arrows indicate the truncated oxidized acyl chains whereas the green circles indicate the presence of multiple fatty acid chains.